2013 International Nuclear Atlantic Conference - INAC 2013
Recife, PE, Brazil, November 24-29, 2013
ASSOCIAÇÃO BRASILEIRA DE ENERGIA NUCLEAR - ABEN
ISBN: **978-85-99141-05-2**

ANALYSIS OF TRISO PACKING FRACTION AND FISSILE MATERIAL TO DB-MHR USING LWR REPROCESSED FUEL

Clarysson A. M. da Silva[1], Claubia Pereira[1,2] , Antonella L. Costa[1,2], Maria Auxiliadora F. Veloso[1,2] and Maritza R. Gual[1,3].

[1] Departamento de Engenharia Nuclear, Universidade Federal de Minas Gerais, Av. Antônio Carlos, 6627 – Campus UFMG, PCA1 – Anexo Engenharia – Pampulha, CEP 31270-901 Belo Horizonte, MG.
clarysson@nuclear.ufmg.br, claubia@nuclear.ufmg.br, antonella@nuclear.ufmg.br, dora@nuclear.ufmg.br

[2] Instituto Nacional de Ciências e Tecnologia de Reatores Nucleares Inovadores/CNPq
http://www.cnpq.br/programas/inct/_apresentacao/inct_reatores_nucleares.html

[3] Instituto Superior de Ciencias y Tecnologías Avanzadas (InsTEC), Departamento de Ingeniería Nuclear, Av. Salvador Allende y Luaces, CP 10300, La Habana, Cuba
maritzargual@gmail.com

ABSTRACT

Gas-cooled and graphite-moderated reactor is being considered the next generation of nuclear power plants because of its characteristic to operate with reprocessed fuel. The typical fuel element consists of a hexagonal block with coolant and fuel channels. The fuel pin is manufactured into compacted ceramic-coated particles (TRISO) which are used to achieve both a high burnup and a high degree of passive safety. This work uses the MCNPX 2.6.0 to simulate the active core of Deep Burn Modular Helium Reactor (DB-MHR) employing PWR (Pressurized Water Reactor) reprocessed fuel. However, before a complete study of DB-MHR fuel cycle and recharge, it is necessary to evaluate the neutronic parameters to some values of TRISO Packing Fractions (PF) and Fissile Material (FM). Each PF and FM combination would generate the best behaviour of neutronic parameters. Therefore, this study configures several PF and FM combinations considering the heterogeneity of TRISO layers and lattice. The results present the best combination of PF and FM values according with the more appropriated behaviour of the neutronic parameters during the burnup. In this way, the optimized combination can be used to future works of MHR fuel cycle and recharge.

1. INTRODUCTION

Brazil participates in the group of countries that are developing searchers to new-generation reactor designs and systems. The gas-cooled and graphite-moderated reactors may be the next generation of nuclear systems because of its characteristic to operate with several different types of fuel (Light Water Reactors (LWR) wastes, military plutonium or thorium). The Deep Burn Modular Helium Reactor (DB-MHR) proposed by the General Atomics Company utilizes reprocessed LWR spent fuel where the recovered isotopes (Pu, Np, Am and Cm) are used to fabricate fresh fuel. These fuels are manufactured into ceramic-coated particles [tristructural-isotropic (TRISO)] which are used to achieve high burnup and high degree of passive safety. These particles are compacted with graphite powder to form fuel pin which can have several values of TRISO packing fraction (PF). Previous studies have evaluated the influence of PF in the neutronic parameters to gas-cooled and graphite-moderated reactors [1, 2]. In this way, the present work analyzes both variations of PF and Fissile Material (FM) values. Each PF value is associated with FM values. The goal is evaluate the effective multiplication factor (k_{eff}) and the fuel composition variation during the burnup to each PF-FM combination. To simulate the DB-MHR core, the MCNPX 2.6.0 (Monte Carlo N-Particle

transport eXtended code version 2.6.0) was used and the models consider the heterogeneity of TRISO layers and lattice.

2. METHODOLOGY

2.1. Geometry Reactor Descriptions

The DB-MHR geometry is similar to a typical MHR design. The core has a cylindrical geometry with 4 m radius and 10 m high, filled by 13 x 13 matrixes of hexagonal blocks containing fuel and graphite. The active core consists of three concentric rings with 108 hexagonal fuel blocks with 20.8 cm side and 7.93m height. These fuel blocks are filled with 108 coolant channels and 216 fuel channels with radius of 0.797cm and 0.635 cm, respectively. The fuel channels contain fuel pins with radius of 0.662 cm where each fuel block has 216 fuel pins. Reflectors with 1.035 m high cover the top and bottom of the core. The DB-MHR fuel form is TRISO (Tristructural-isotropic). TRISOs are small spherical fuel (namely kernel) coated by 4 layers being: porous carbon, pyrocarbon, silicon carbide and pyrocarbon. These particles are compacted with powder graphite to manufacture the fuel pins [3, 4, 5, 6, 7, 8 and 9]. Fig. 1 illustrates the design of core, fuel blocks and TRISO particles. In addition, Table I presents the main core design parameters of the simulated reactor and Table II presents information about the dimensions and the material to TRISO particle.

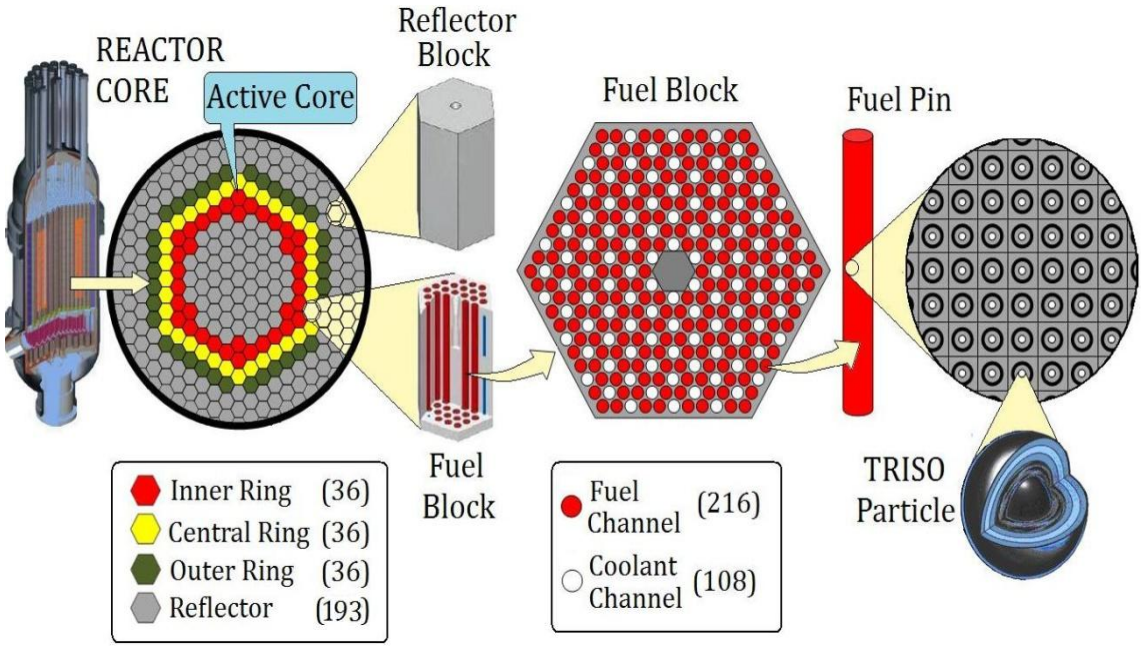

Figure 1: Schematic representation of DB-MHR core.

Table 1: Major design parameters of the simulated reactor

Description (unity)	Value
Thermal power (MWt)	600.0
Coolant inlet temperature (ºC)	490.0
Coolant outlet temperature (ºC)	850.0
Power density (W/cm^3)	6.210
Number of fuel columns	108.0
Active core height (cm)	793.0
Total core height (cm)	1000.0
Core radius (cm)	400.0
Graphite block density (g/cm^3)	1.740
Fuel block side (cm)	20.78
Number of coolant channels in each fuel block	108.0
Number of fuel channels in each fuel block	216.0
Number of fuel pins in each fuel block	216.0
Fuel pin radius (cm)	0.622
Fuel pin height (cm)	793.0
Fuel pitch distance (cm)	1.880
Fuel channel radius (cm)	0.6350
Coolant channel radius (cm)	0.7970

Table 2: TRISO particle structure of the simulations

Material	Radius (μm)	Density (g/cm^3)
Kernel	1.500 10^2	10.20
Porous carbon	3.000 10^2	1.00
Pyrocarbon	3.350 10^2	1.85
Silicon carbide	3.700 10^2	3.20
Pyrocarbon	4.100 10^2	1.85

2.2. The Simulated Geometry

The Fig. 2 and Fig. 3 show, respectively, the radial and axial view of the reactor core simulated in the MCNPX 2.6.0 code. It was modelled using the actual dimensions of DB-MHR (see Table 1) where the number and dimensions of fuel blocks, fuel pins, coolant channels and TRISOs particles are in agreement with the DB-MHR feature. The core was represented by a cylinder filled with hexagonal fuel blocks and reflector blocks (see Fig.2). In the axial view the core has 7.93 m of fuel block and 1.035 m of superior and inferior graphite reflector (see Fig. 3). In the radial view the core there are three zones: central reflector, active core and outer reflector. The active core consists of three concentric rings that contain 108 fuel blocks. Each ring has 36 fuel blocks and, therefore, the fuel volume is the same in the three rings. Inside each fuel block there is a hexagonal lattice that has 108 coolant channels and 216 fuel channels. The Fig. 2 also illustrates the fuel block geometry used to perform the simulations with the hexagonal lattice and the positions of fuel and coolant channels.

Inside of fuel channels are the fuel pins which contain TRISOs particles. The simulated models present fuel pins with TRISOs spheres equally spaced by square lattice (see Fig. 2).

These small particles were configured with the fuel kernel and the four graphite layers where the dimensions and the material density are according with Table 2 (see Fig. 4). Therefore, this study considers the TRISOs granularity in the fuel pin and the heterogeneity of the TRISOs particles.

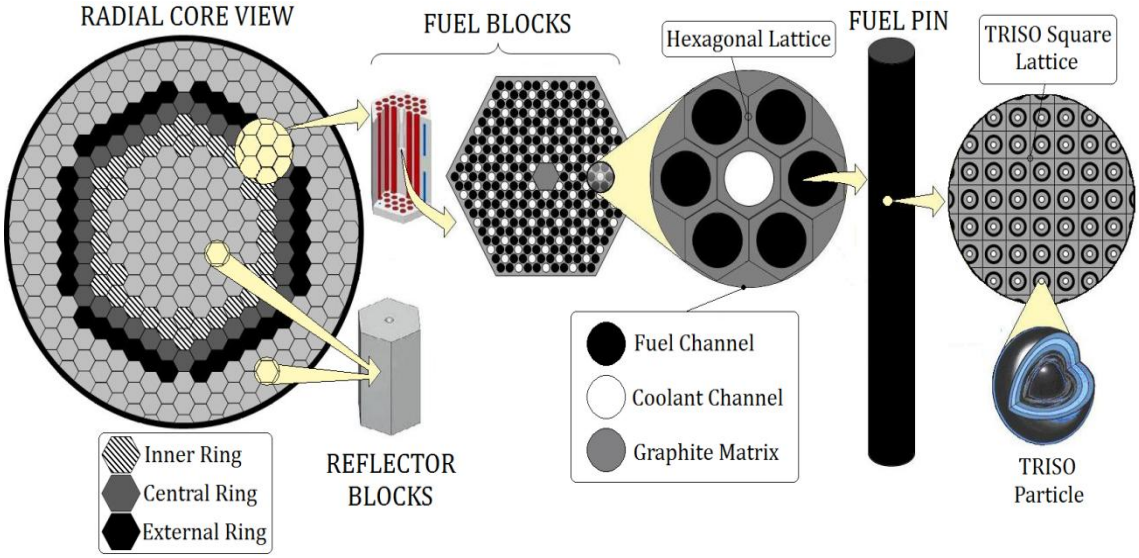

Figure 2: Radial view of DB-MHR in the MCNPX 2.6.0 configuration.

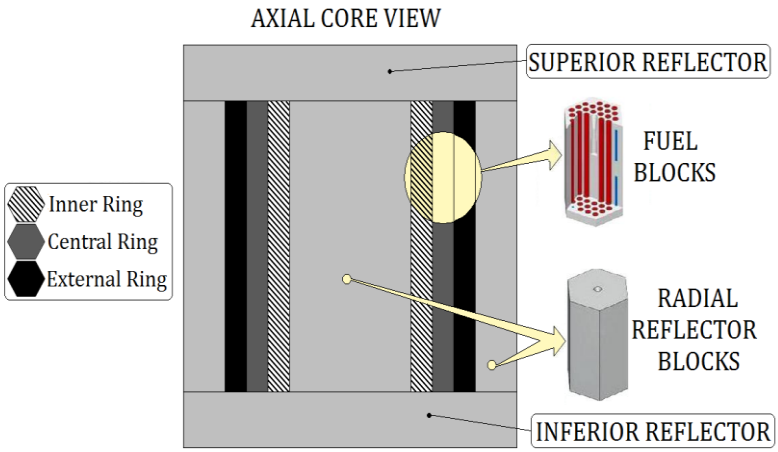

Figure 3: Axial view of DB-MHR in the MCNPX 2.6.0 configuration.

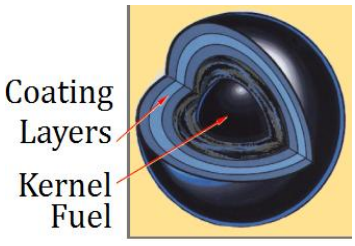

Layer	Material
1st	Porous Carbon
2nd	Pyrocarbon
3rd	Silicon Carbide
4th	Pyrocarbon

Figure 4: Configuration of TRISO particles in MCNPX 2.6.0 core.

2.3. TRISO Pitch Distance and Packing Fraction Relation

The quantity of TRISO particles inside a fuel pin is associated with PF concept. If the fuel pin, the radius does not change, the PF variations are correlated with the alterations in the distance between TRISO particles (TRISO pitch distance). In the simulations, nine PF values were evaluated considering previous studies [1]. Thus, the TRISO Pitch Distance (PD) was calculated to match these specific PF values (see Table 3) using the following equation:

$$PD = \left[\frac{\text{TRISO volume}}{PF}\right]^{\frac{1}{3}} \quad (1)$$

Considering constant the fuel pin radius, to increase the PF values, the quantity of TRISO particles must increase and the TRISO PD decrease. This characteristic can be seen by equation (1) where the values of PF and PD are inversely proportional (see Table 3).

Table 3: Relation between Pith Distance (PD) and Packing Fraction (PF)

PD (cm)	PF
$1.130\ 10^{-1}$	$2.000\ 10^{-1}$
$1.049\ 10^{-1}$	$2.500\ 10^{-1}$
$9.873\ 10^{-2}$	$3.000\ 10^{-1}$
$9.378\ 10^{-2}$	$3.500\ 10^{-1}$
$8.970\ 10^{-2}$	$4.000\ 10^{-1}$
$8.625\ 10^{-2}$	$4.500\ 10^{-1}$
$8.327\ 10^{-2}$	$5.000\ 10^{-1}$
$8.067\ 10^{-2}$	$5.500\ 10^{-1}$
$7.836\ 10^{-2}$	$6.000\ 10^{-1}$

2.4. Fuel Composition and Fuel Cycle

The DB-MHR fuels can have high enrichment values. However, due to the proliferation risks, Fissile Material (FM) should be limited to 20%. In this way, three FM percentages were evaluated: 10, 15 and 20% (Table 4). In the simulations, the initial fuel composition was based on a theoretical cycle to manufacture the Fresh Fuel (FF) as represented in the Fig. 5. This fuel is a mix of Natural Uranium (NU) and Reprocessed Material (RM) which consists of isotopes (Pu and MAs) recovered by UREX+ method [10]. In the fuel fabrication plant the RM is spiked with NU to fabricate the FF where each FM value has different concentration of RM and NU, as shown in the Table 4. The composition of the Spent Fuel (SF) was obtained using the ORIGEN 2.1 code [11] from a burned PWR standard fuel (33,000 MWd/tHM burned), with 3.1% of initial enrichment, which was remained in the cooling pool for five years.

The DB-MHR core was simulated without reloaded using only one cycle step.

Table 4: Weight Fraction Fuel Composition with Reprocessed Material (RM) and Natural Uranium (NU) concentrations

Isotope	Fissile Material (FM) percentage		
	10 %	15 %	20 %
^{235}U	$5.241\ 10^{-3}$	$4.741\ 10^{-3}$	$4.240\ 10^{-3}$
^{238}U	$7.434\ 10^{-1}$	$6.725\ 10^{-1}$	$6.015\ 10^{-1}$
^{237}Np	$4.373\ 10^{-3}$	$6.725\ 10^{-3}$	$9.077\ 10^{-3}$
^{238}Pu	$2.316\ 10^{-3}$	$3.562\ 10^{-3}$	$4.807\ 10^{-3}$
^{239}Pu	$6.759\ 10^{-2}$	$1.039\ 10^{-1}$	$1.403\ 10^{-1}$
^{240}Pu	$2.835\ 10^{-2}$	$4.359\ 10^{-2}$	$5.883\ 10^{-2}$
^{241}Pu	$1.532\ 10^{-2}$	$2.356\ 10^{-2}$	$3.180\ 10^{-2}$
^{242}Pu	$8.067\ 10^{-3}$	$1.240\ 10^{-2}$	$1.674\ 10^{-2}$
^{241}Am	$4.688\ 10^{-3}$	$7.209\ 10^{-3}$	$9.729\ 10^{-3}$
^{242}Am	$1.254\ 10^{-5}$	$1.928\ 10^{-5}$	$2.602\ 10^{-5}$
^{243}Am	$1.760\ 10^{-3}$	$2.707\ 10^{-3}$	$3.654\ 10^{-3}$
^{242}Cm	$1.017\ 10^{-7}$	$1.563\ 10^{-7}$	$2.110\ 10^{-7}$
^{243}Cm	$5.401\ 10^{-6}$	$8.305\ 10^{-6}$	$1.121\ 10^{-5}$
^{244}Cm	$4.060\ 10^{-4}$	$6.243\ 10^{-4}$	$8.426\ 10^{-4}$
^{245}Cm	$2.139\ 10^{-5}$	$3.290\ 10^{-5}$	$4.440\ 10^{-5}$
^{246}Cm	$2.753\ 10^{-6}$	$4.234\ 10^{-6}$	$5.714\ 10^{-6}$
O_2	$1.184\ 10^{-1}$	$1.184\ 10^{-1}$	$1.184\ 10^{-1}$
RM	$2.514\ 10^{-1}$	$3.228\ 10^{-1}$	$3.943\ 10^{-1}$
NU	$7.486\ 10^{-1}$	$6.772\ 10^{-1}$	$6.057\ 10^{-1}$

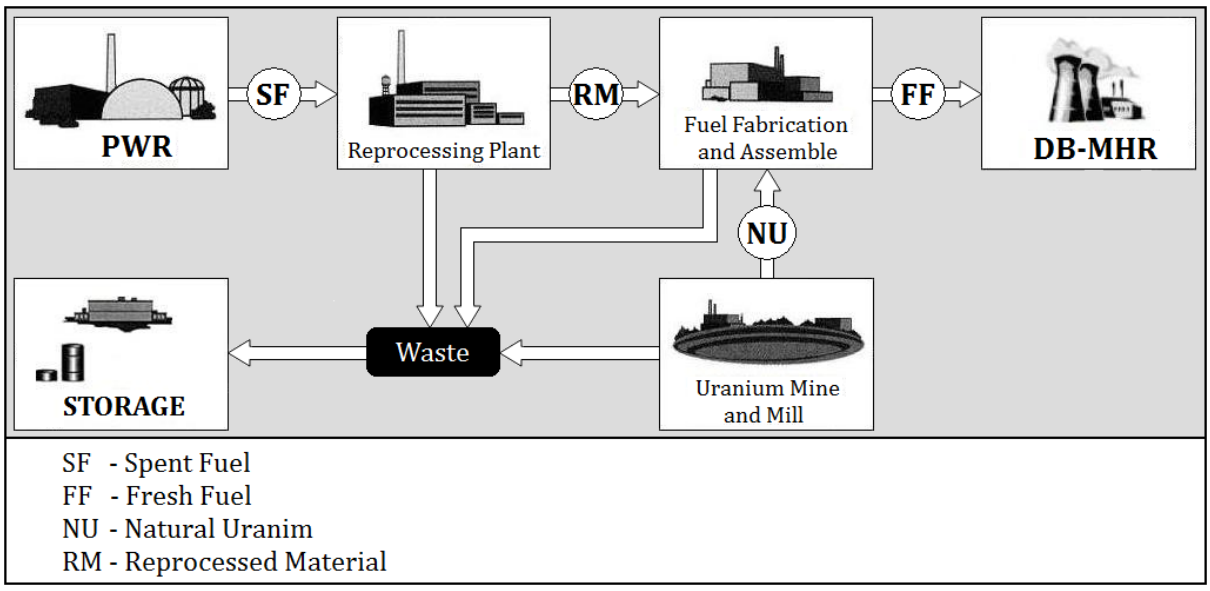

Figure 5: Theoretical (RM+NU) fuel cycle.

2.5. Burnup Information

The depletion evaluation will consider the specific power density of DB-MHR (250 W/g) with time steps of 30 days where the cell temperature will be adjusted to the reactor temperature at full power. The MCNPX 2.6.0 depletion is a linked process involving steady-state flux calculations by the MCNPX and nuclide depletion calculations by CINDER90. MCNPX runs a steady-state calculation to determine the system eigenvalue, 63-group fluxes, energy-integrated reaction rates, fission multiplicity (ν), and recoverable energy per fission (Q values). CINDER90 then takes those MCNPX generated values and performs the depletion calculation to generate new number densities for the next time step. MCNPX takes these new number densities and generates another set of fluxes and reaction rates. The process repeats itself until after the final time step specified by the user. The MCNPX 2.6.0 uses the ENDF-VI.6 to steady-state flux calculations and the CINDER.dat library to depletion calculation by CINDER90. The CINDER.dat library file includes isotope decay and interaction probability data for 3400 isotopes including, ~30 fission yield sets, and yield data for 1325 fission products [12].

2.6. Evaluated Cases

To analyze nine TRISO packing fractions (Table 3) with three different compositions (Table 4), twenty-seven combinations were configured (see Table 5). Therefore, twenty-seven cases were simulated where each PF has three FM percentages (10, 15 and 20%). The nomenclature to the combinations is "Case FM-PF" where two first digits represent the FM and the last two digits represent the PF value.

Table 5: Evaluated Cases Nomenclature

FM percentage	Packing Fraction (PF)								
	20%	25%	30%	35%	40%	45%	50%	55%	60%
10%	1020	1025	1030	1035	1040	1045	1050	1055	1060
15%	1520	1525	1530	1535	1540	1545	1550	1555	1560
20%	2020	2025	2030	2035	2040	2045	2050	2055	2060

3. RESULTS

Initially the DB-MHR core was simulated in steady-state condition where the k_{eff} was evaluated to all FM-PF combinations at beginning of cycle. Fig. 6 shows the k_{eff} to each FM-PF combinations where each curve represent a Fissile Material (FM) percentage. Of course, 10% of FM has the lowest k_{eff} and 20% of FM has the biggest k_{eff} values. The highest enrichment generates more thermal fission that generates biggest k_{eff} value. Also, the three curves present the same shape. The k_{eff} increases as the PF augments because the quantity of TRISO fuel is proportional to PF values. The k_{eff} variation is bigger between 20 and 40% of PF values but between 40 and 60% of PF there are small k_{eff} variations.

Considering the first results presented in the Fig. 6, highest values of k_{eff} were chosen to evaluate the burnup. Then, the values 15 and 20% of FM and 40 up to 60% of PF were selected. These values correspond to ten cases: 1540, 1545, 1550, 1555, 1560, 2040, 2045,

2050, 2055 and 2060 (see Table 5). Therefore, only these cases will be considered in the next analyzes.

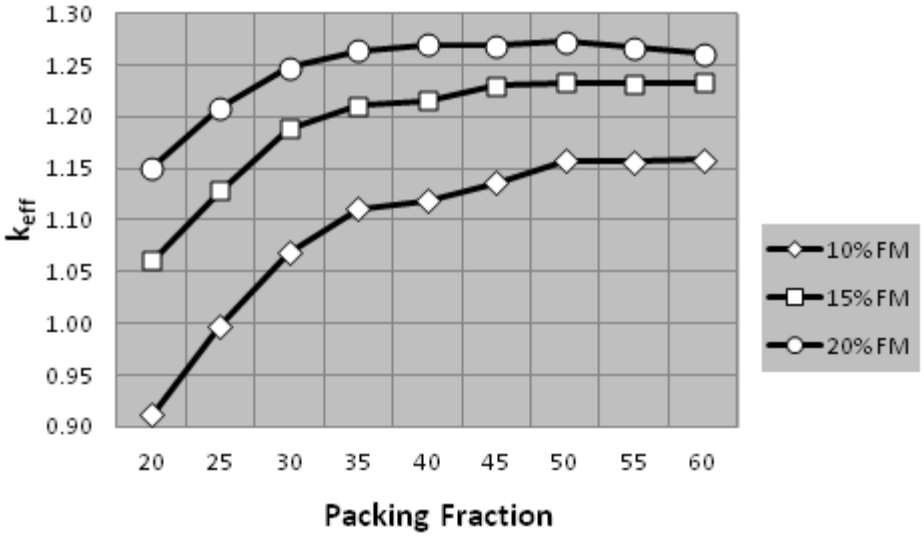

Figure 6: Initial k_{eff} versus Packing Fraction.

The Fig. 7 and 8 show the k_{eff} behaviour during the 300 days of full reactor operation to cases with 15 and 20 % of FM respectively.

Among the studied cases, the k_{eff} has the smallest value to 40 % of PF at end of cycle. But, to 50, 55 and 60 % of PF there is not significant k_{eff} difference (see Fig. 7 and 8) during the burnup. At the end of the cycle, these differences are around 0.001. This behaviour is in agreement with the Fig. 6 that shows small variations among 50, 55 and 60 % of PF values at begging of cycle.

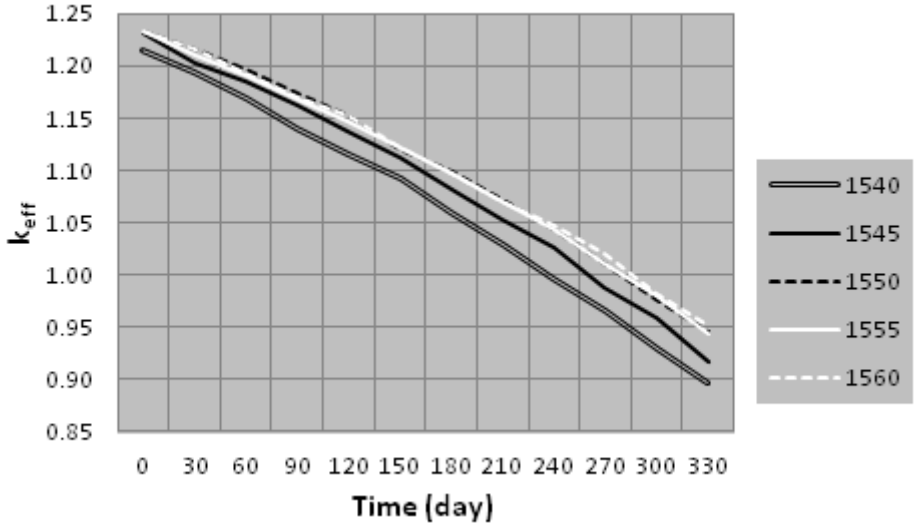

Figure 7: Effective Multiplication Factor during burnup to 15% of FM

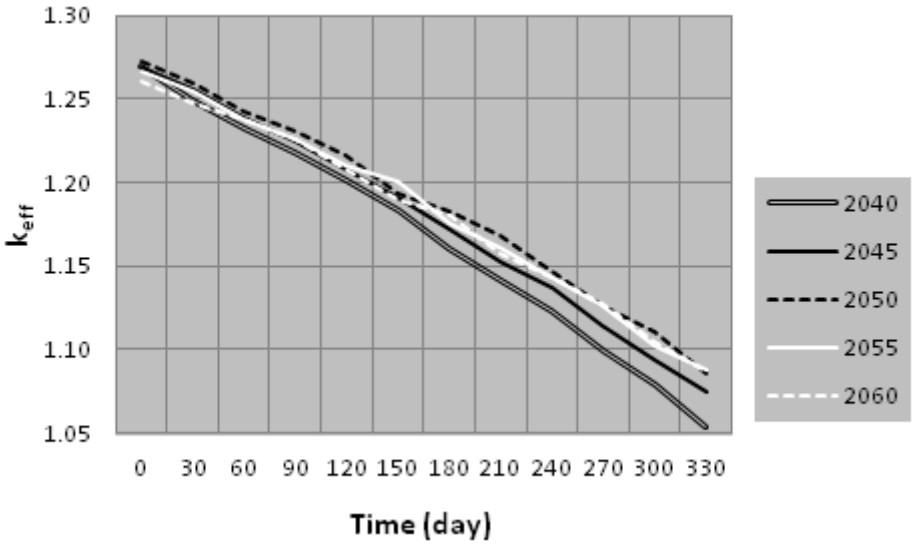

Figure 8: Effective Multiplication Factor during burnup to 20% of FM

Table 6 and 7 present the Weight Fraction Variation (WFV) of the fuel composition for 15 and 20% of FM respectively. This WFV was calculated by the difference:

$$\mathrm{WFV}=\mathrm{WF(BOC)}-\mathrm{WF(EOC)} \tag{2}$$

where WF(BOC) is the weight fraction at beginning of cycle and WF(EOC) is the weight fraction at end of cycle.

Table 6: WFV of the fuel composition during the DB-MHR cycle to 15% FM

Isotopes	Cases				
	1540	1545	1550	1555	1560
^{235}U	$-2.011\ 10^{-3}$	$-1.985\ 10^{-3}$	$-1.964\ 10^{-3}$	$-1.949\ 10^{-3}$	$-1.936\ 10^{-3}$
^{238}U	$3.022\ 10^{-2}$	$2.982\ 10^{-2}$	$2.942\ 10^{-2}$	$2.932\ 10^{-2}$	$2.902\ 10^{-2}$
^{237}Np	$-8.980\ 10^{-4}$	$-9.050\ 10^{-4}$	$-9.150\ 10^{-4}$	$-9.140\ 10^{-4}$	$-9.190\ 10^{-4}$
^{238}Pu	$8.621\ 10^{-4}$	$9.051\ 10^{-4}$	$9.471\ 10^{-4}$	$9.601\ 10^{-4}$	$9.841\ 10^{-4}$
^{239}Pu	$-6.513\ 10^{-2}$	$-6.485\ 10^{-2}$	$-6.462\ 10^{-2}$	$-6.445\ 10^{-2}$	$-6.430\ 10^{-2}$
^{240}Pu	$4.101\ 10^{-3}$	$3.581\ 10^{-3}$	$3.171\ 10^{-3}$	$3.221\ 10^{-3}$	$2.891\ 10^{-3}$
^{241}Pu	$-5.821\ 10^{-3}$	$-5.311\ 10^{-3}$	$-4.891\ 10^{-3}$	$-4.841\ 10^{-3}$	$-4.551\ 10^{-3}$
^{242}Pu	$7.615\ 10^{-3}$	$7.575\ 10^{-3}$	$7.545\ 10^{-3}$	$7.485\ 10^{-3}$	$7.485\ 10^{-3}$
^{241}Am	$-2.995\ 10^{-3}$	$-2.995\ 10^{-3}$	$-2.999\ 10^{-3}$	$-2.989\ 10^{-3}$	$-2.987\ 10^{-3}$
^{242}Am	$-2.111\ 10^{-6}$	$-1.961\ 10^{-6}$	$-1.821\ 10^{-6}$	$-1.731\ 10^{-6}$	$-1.671\ 10^{-6}$
^{243}Am	$6.430\ 10^{-4}$	$7.050\ 10^{-4}$	$7.410\ 10^{-4}$	$7.580\ 10^{-4}$	$7.850\ 10^{-4}$
^{242}Cm	$1.755\ 10^{-3}$	$1.758\ 10^{-3}$	$1.762\ 10^{-3}$	$1.758\ 10^{-3}$	$1.759\ 10^{-3}$
^{243}Cm	$1.244\ 10^{-5}$	$1.270\ 10^{-5}$	$1.303\ 10^{-5}$	$1.309\ 10^{-5}$	$1.327\ 10^{-5}$
^{244}Cm	$5.687\ 10^{-4}$	$6.027\ 10^{-4}$	$6.357\ 10^{-4}$	$6.407\ 10^{-4}$	$6.607\ 10^{-4}$
^{245}Cm	$-1.551\ 10^{-5}$	$-1.371\ 10^{-5}$	$-1.203\ 10^{-5}$	$-1.129\ 10^{-5}$	$-1.008\ 10^{-5}$
^{246}Cm	$6.576\ 10^{-6}$	$6.756\ 10^{-6}$	$6.936\ 10^{-6}$	$6.976\ 10^{-6}$	$7.076\ 10^{-6}$

Table 7: WFV of the fuel composition during the DB-MHR cycle to 20% FM

Isotopes	Cases				
	2040	2045	2050	2055	2060
^{235}U	-1.223 10^{-3}	-1.203 10^{-3}	-1.182 10^{-3}	-1.181 10^{-3}	-1.169 10^{-3}
^{238}U	2.776 10^{-2}	2.726 10^{-2}	2.686 10^{-2}	2.686 10^{-2}	2.656 10^{-2}
^{237}Np	-7.216 10^{-4}	-7.386 10^{-4}	-7.536 10^{-4}	-7.626 10^{-4}	-7.696 10^{-4}
^{238}Pu	1.180 10^{-3}	1.239 10^{-3}	1.293 10^{-3}	1.312 10^{-3}	1.341 10^{-3}
^{239}Pu	-6.819 10^{-2}	-6.793 10^{-2}	-6.758 10^{-2}	-6.778 10^{-2}	-6.755 10^{-2}
^{240}Pu	7.42810^{-3}	6.818 10^{-3}	6.238 10^{-3}	6.218 10^{-3}	5.908 10^{-3}
^{241}Pu	-5.200 10^{-3}	-4.490 10^{-3}	-3.830 10^{-3}	-3.740 10^{-3}	-3.370 10^{-3}
^{242}Pu	7.377 10^{-3}	7.307 10^{-3}	7.227 10^{-3}	7.227 10^{-3}	7.187 10^{-3}
^{241}Am	-2.569 10^{-3}	-2.580 10^{-3}	-2.584 10^{-3}	-2.602 10^{-3}	-2.601 10^{-3}
^{242}Am	4.067 10^{-6}	4.447 10^{-6}	4.877 10^{-6}	4.917 10^{-6}	5.167 10^{-6}
^{243}Am	7.094 10^{-4}	7.744 10^{-4}	8.184 10^{-4}	8.404 10^{-4}	8.624 10^{-4}
^{242}Cm	1.800 10^{-3}	1.809 10^{-3}	1.814 10^{-3}	1.822 10^{-3}	1.824 10^{-3}
^{243}Cm	8.461 10^{-6}	8.911 10^{-6}	9.301 10^{-6}	9.461 10^{-6}	9.641 10^{-6}
^{244}Cm	5.844 10^{-4}	6.274 10^{-4}	6.684 10^{-4}	6.824 10^{-4}	7.004 10^{-4}
^{245}Cm	-1.442 10^{-5}	-1.192 10^{-5}	-9.039 10^{-6}	-8.159 10^{-6}	-6.399 10^{-6}
^{246}Cm	6.796 10^{-6}	6.916 10^{-6}	7.046 10^{-6}	7.096 10^{-6}	7.166 10^{-6}

The WFV presents same behaviour to the evaluated cases. For 15% of FM (Table 6) there are weight fraction reduction to isotopes ^{235}U, ^{237}Np, ^{239}Pu, ^{241}Pu, ^{241}Am, ^{242}Am and ^{245}Cm. On the other hand, there is weight fraction increase to isotopes ^{238}U, ^{238}Pu, ^{240}Pu, ^{242}Pu, ^{243}Am, ^{242}Cm, ^{243}Cm, ^{244}Cm and ^{246}Cm. As ^{235}U, ^{239}Pu and ^{241}Pu are fissile isotopes; their reduction during the burnup is expected. The decrease of ^{237}Np, ^{241}Am, ^{242}Am and ^{245}Cm can be due its transmutation into respective isotopes ^{238}Pu, ^{242}Cm, ^{243}Cm and ^{246}Cm. Table 6 shows inverse behaviour between ^{237}Np and ^{238}Pu, ^{241}Am and ^{242}Cm, ^{242}Am and ^{243}Cm, ^{245}Cm and ^{246}Cm. For example, to ^{237}Np, the WFV reduces while to ^{238}Pu this value increases to all studied cases. Table 7 shows similar behaviour of Table 6 except to ^{242}Am which presents weight fraction increased.

Analysing the composition and considering the isotopes of an element, there is gradual variation of weight fraction as the PF increase (see Table 6 and 7). The PF value is associated with TRISO quantity inside the fuel pin and therefore it is associated with the fuel volume. Thus, the Cases 1560 and 2060 have the biggest fuel volume. The isotopic depletion during the burnup depends of the fuel volume. As the specific power density is the same to all evaluated cases, the biggest fuel volume case will correspond to the smallest depletion of fissile isotopes ^{235}U, ^{239}Pu and ^{241}Pu. This behaviour can be noted by Table 6 and 7. For example, to isotope ^{235}U, the WFV is -2.011×10^{-3} to the Case 1540 (40% PF), but it is -1.936×10^{-3} to the Case 1560 (60%PF). On the other hand, the transmutation of ^{237}Np into ^{238}Pu presents an inverse behaviour. The 60% PF cases have the biggest reduction of ^{237}Np and the biggest increase of ^{238}Pu. In this way, the Cases 1560 and 2060 have the biggest transmutation of ^{237}Np into ^{238}Pu (see Table 6 and 7). For example, the reduction of ^{237}Np is -8.980×10^{-4} to Case 1540 (40% PF) and -9.190×10^{-4} to Case 1560 (60% PF). Instead, the increase of ^{238}Pu is 8.621×10^{-4} to Case 1540 (40% PF) and 9.841×10^{-4} to Case 1560 (60% PF).

4. CONCLUSIONS

In the steady-state analysis, k_{eff} presents the smallest values to all cases of 10% of FM and to all cases of 20, 25, 30 and 35% of PF. Thus, to extend burnup analysis, these cases were not evaluated. In this analysis the cases of 15 and 20% of FM combined with 40, 45, 50, 55 and 60% PF were studied. The cases with 20% of FM presented biggest k_{eff} values during the burnup, as expected. For the same FM value, the cases with 50, 55 and 60% of PF presented small k_{eff} differences and have the biggest k_{eff} values at the end of cycle. Thus, considering less fuel utilization in the fabrication process, 50% of PF would be used to DB-MHR burnup. The 15% of FM is sufficient to 330 days of reactor cycle. On the other hand, to provide an extended burnup it would be necessary 20% of FM.

Analysing the composition and considering the isotopes of an element, there is gradual weight fraction variation as the PF value increase. For the evaluated cases, it is observed a weight fraction reduction to isotopes ^{235}U, ^{237}Np, ^{239}Pu, ^{241}Pu, ^{241}Am and ^{245}Cm while there are weight fraction increase to isotope ^{238}U, ^{238}Pu, ^{240}Pu, ^{242}Pu, ^{243}Am, ^{242}Cm, ^{243}Cm, ^{244}Cm and ^{246}Cm.

The temperature coefficients analysis is necessary to ensure adequate safety parameters values. In this way, future works will be performed using MCNPX 2.6.0 and other nuclear codes (e.g. SCALE – Standardized Computer Analyses for Licensing Evaluation code system and/or WIMS – Winfrith Improved Multi/group Scheme) to compare the results.

ACKNOWLEDGMENTS

The authors are grateful to the Brazilian research funding agencies, CNEN (Brazil), CNPq (Brazil), CAPES (Brazil) and FAPEMIG (MG/Brazil), for the support.

REFERENCES

1. F. C. Silva, *Avaliação Neutrônica da Inserção de Transurânicos em Reatores Nucleares Tipo VHTR*, Universidade Federal de Minas Gerais - Master Thesis, Belo Horizonte, Brazil (2012).
2. F. C. Silva, C. Pereira, M. A. F. Veloso and A. L. Costa, "Shifting study of a VHTR using reprocessed fuel with various TRISO packing fractions", *Nuclear Engineering and Design*, **Volume 248**, pp.42-47 (2012).
3. A. Talamo, "Prediction of TRISO Coated Particle Performances for a One-pass Deep Burn," *Journal of Material Nuclear*, **Volume 373**, pp. 407–414 (2008).
4. A. Talamo, "Managing the Reactivity Excess of Gas Turbine-Modular Helium Reactor by Burnable Poison and Control Rods," *Annals of Nuclear Energy*, **Volume 33**, pp. 84–98 (2005).

5. A. Talamo, W. Gudowski and and F. Venneri, “The burnup capabilities of Deep Burn Modular Helium Reactor Analyzed by the Monte Carlo Continuous Energy Code MCB,” *Annals of Nuclear Energy*, **Volume 31**, pp. 173-196 (2003).
6. R. Plukienea and D. Ridikas, “Modelling of HTRs with Monte Carlo: from a homogeneous to an exact heterogeneous core with microparticles,” *Annals of Nuclear Energy*, **Volume 30,** pp. 1573-1585 (2003).
7. A. Talamo, W. Gudowski, J. Cetnar and F. Venneri, “Key Physical Parameters and Temperature Reactivity Coefficients of the Deep Burn Modular Helium Reactor Fueled with LWRs waste,” *Annals of Nuclear Energy*, **Volume 31**, pp. 1913-1937 (2004).
8. D. Wongsawaeng, “Performance modeling of Deep Burn TRISO fuel using ZrC as a load-bearing layer and an oxygen getter,” *Journal of Nuclear Materials*, **Volume 396**, pp. 149-158 (2010).
9. A. Talamo, W. Gudowski, “A Deep Burn Fuel Management Strategy for the Incineration of Military Plutonium in the Gas Turbine–Modular Helium Reactor Modeled in a Detailed Three-Dimensional Geometry by the Monte Carlo Continuous Energy Burnup Code,” *Nuclear Science and Engineering.* **Volume 153**, pp. 172-184 (2006).
10. G. F. Vandergrift, et al. “Lab-scale demonstration of the UREX+ process.” *Proceeding 4th WM Conference*. Tucson. pp.1-10 (2004).
11. Croff, A. G., *A User's Manual for the ORIGEN2 Computer Code*, Oak Ridge National Laboratory, Report ORNL/TM-7175 (1980).
12. J. S. Hendricks, et al. *MCNPX 2.6.0 Manual Extensions*, Los Alamos National Laboratory, Report LA-UR-08-2216 (2008).